

# Metabolic flux from the chloroplast provides essential signals for retrograde signalling during cold acclimation

Helena Herrmann<sup>1</sup>, Beth Dyson<sup>2</sup>, Matthew Miller<sup>1</sup>, Jean Marc Schwartz<sup>1</sup>, and Giles N. Johnson<sup>1</sup>

<sup>1</sup>University of Manchester

<sup>2</sup>University of Sheffield

May 5, 2020

## Abstract

Chloroplasts, the site of the primary reactions of photosynthesis, are organelles capable of independent protein synthesis, but which depend on the nucleus for most polypeptides. The process of photosynthesis is especially sensitive to environmental conditions and the composition of the photosynthetic apparatus can be modulated in response to environmental change. This acclimation process requires close communication between chloroplast and nucleus. Here we present evidence that the form in which carbon is exported from the chloroplast encodes information about the metabolic status of the photosynthetic apparatus which in turn controls photosynthetic acclimation.

## Authorship:

Gas exchange measurements were carried out by BCD and HAH. Metabolite assays were conducted by BCD. The proteomics data was generated and analysed by MAEM. Metabolic modelling and network analyses were done by HAH. GNJ conceived the idea and wrote the manuscript. HAH and JMS edited the manuscript. All authors reviewed the manuscript.

**Acknowledgements:** We would like to thank Drs David Knight, Ronan O’Cualain and Julian Selley for their help with the proteomic analysis. This work was supported by a grant from the Biotechnology and Biological Sciences Research Council (BBSRC; BB/J04103/1). HAH and MAEM were supported BBSRC studentships (BB/M011208/1).

**Conflict of Interest Statement:** the authors declare they have no conflicts of interest in relation to this work.

**Keywords:** acclimation, carbon metabolism, cold, fumarate, malate, photosynthesis

## Introduction

Through their lifecycle, plants experience environmental conditions that vary on timescales from seconds to seasons. *Arabidopsis thaliana* is typically a winter annual, germinating in the autumn and persisting through the winter, prior to flowering in spring (Grime *et al.*, 1988). Across this time-period, mean daily temperatures may vary by 20°C or more. To optimise survival and growth, plants acclimate to changes in temperature, altering their investment in different processes to suit the conditions experienced (Ruelland, Vaultier, Zachowski, & Hury, 2009; Walters, 2005). The process of acclimation can involve both structural changes, with tissues differing when developed in different conditions, but also relatively rapid (days-weeks) dynamic responses, which tracks changes in the environment (Athanasίου, Dyson, Webster, & Johnson,

2010; Walters, 2005). Changes in both light intensity and temperature are known to trigger acclimation (Athanasidou *et al.*, 2010; Dyson *et al.*, 2015; Dyson *et al.*, 2016; Huner *et al.*, 1993; Savitch *et al.*, 2001; Stitt & Hurry, 2002; Strand, Hurry, Gustafsson, & Gardestrom, 1997; Walters & Horton, 1994).

Exposure to low temperature triggers a complex array of acclimation responses. A significant amount of work in plant cold responses has focused on the acquisition of freezing tolerance (see Knight & Knight, 2012 for a review). In addition, it is recognised that plants can optimise their metabolism to suit changing conditions. For example, acclimation of both photosynthesis (Huner *et al.*, 1993; Strand *et al.*, 1997; Strand *et al.*, 1999) and respiration (Armstrong, Logan, Tobin, O’Toole, & Atkin, 2006; Talts, Pärnik, Gardeström, & Keerbergh, 2004) to low temperature are seen, these being metabolic processes which are easily monitored *in vivo*. A prominent feature of metabolic acclimation is an increase in the capacity of metabolism, with enzyme and metabolite concentrations increasing to compensate for the loss of activity at low temperature. This requires the coordination of gene expression across multiple cellular compartments, including retrograde and/or anterograde signals between the nucleus, chloroplast and mitochondrion (Fey, Wagner, Brautigam, & Pfannschmidt, 2005). To date, little is known about either the sensing or the signalling pathways involved in metabolic acclimation.

Acclimation of photosynthesis to low temperature has previously been studied in a range of species, including Arabidopsis. In the short term, low temperature decreases the rate at which sucrose is synthesised and exported from the leaf, with the enzyme sucrose phosphate synthase (SPS) receiving particular attention. Limitations in flux through SPS result in the accumulation of phosphorylated metabolites (Hurry, Strand, Furbank, & Stitt, 2000). This is thought to lead to depletion of the cellular concentration of inorganic phosphate (Pi) which in turn limits the export of triose phosphates from the chloroplast. This inhibits photosynthesis, as the regeneration of Pi in the chloroplast is necessary for ATP synthesis. Over relatively short periods (days) increased expression of SPS removes the limitation in sucrose synthesis. Hurry *et al.* (2000) provided evidence, based on the responses of different mutants with altered phosphate content, leading to the hypothesis that Pi depletion provided a signal for cold acclimation of SPS content.

Recently, we re-examined the responses of Arabidopsis to low temperature (Dyson *et al.*, 2016). Using non-targeted metabolomics, we identified the diel accumulation of the organic acid fumaric acid (predominantly present in the anionic form, fumarate) as important in the response to cold. We showed that the accumulation of fumarate, which requires the presence of a cytosolic isoform of the enzyme fumarase (Pracharoenwattana *et al.*, 2010), is a specific response to temperature. Plants of a mutant lacking this enzyme, *fum2*, not only failed to accumulate fumarate over the photoperiod, they also accumulated *higher* concentrations of phosphorylated intermediates. Crucially, whilst wild-type Arabidopsis plants increase photosynthetic capacity in response to low temperature, *fum2* plants do not. This suggests that Pi deficiency alone is not sufficient to trigger photosynthetic acclimation.

Here, we have used a combined metabolic and proteomic approach, together with physiological analyses to dissect the acclimation processes occurring in Arabidopsis in response to low temperature. We focus on dynamic acclimation responses to cold in leaves developed at higher temperature. Our results show that fumarate accumulation is important for a wide range of metabolic acclimation responses to cold. Based on metabolic modelling, constrained using experimental data, we propose that changes in the pathway of carbohydrate export from the chloroplast link to fumarate accumulation at low temperature and provide a mechanism for retrograde signalling from the chloroplast driving acclimation.

## Materials and Methods

### Plant material and growth

Wild type Col-0 seeds were obtained from the Nottingham Arabidopsis Stock Centre. Seeds possessing insertions in the gene At5g50950 encoding cytosolic FUM2 protein (Pracharoenwattana *et al.*, 2010) were kindly provided by Professor Steven Smith (University of Tasmania, Australia). Plants were grown in an SGC120 growth cabinet (Weiss Technik) with an 8-h photoperiod, temperature of 20°C day/16°C night, and irradiance of 100  $\mu\text{mol m}^{-2} \text{s}^{-1}$  provided by warm white fluorescent tubes for 8 weeks in 3-inch pots

containing peat-based compost. After 8 weeks, plants had reached growth stage 1.10 (Boyes *et al.* , 2001), with more than 10 leaves  $> 1$  mm and persisted without development of flowers until 10 to 12 weeks. Plants for cold treatment were transferred to a similar cabinet at 4°C day/night 1 h prior to the start of the photoperiod. Leaves for metabolite measurements were harvested by flash freezing in liquid nitrogen under growth conditions.

### Measurements of photosynthesis and respiration

Measurements of photosynthetic capacity were made using a LiCor LI-6400 infra-red gas analyser, at a temperature of 20°C in an atmosphere of 2000  $\mu\text{l l}^{-1}$  CO<sub>2</sub> and an irradiance of 2000  $\mu\text{mol m}^{-2} \text{s}^{-1}$  provided by a warm white LED (colour temperature 2800–3200 K). Measurements of photosynthesis and respiration under growth conditions were carried out using the same gas analyser, in the growth cabinet where plants were grown, using ambient air. The gas analyser was placed in the cabinet and allowed to equilibrate for at least 1 hour prior to any measurements. The analyser chamber was placed to give a light intensity in the chamber equivalent to that of plants during growth. Respiration was measured by interrupting illumination, covering the plant and analyser chamber with aluminium foil. Data were analysed using Analysis of Variance, followed by Tukey post-hoc tests in SPSS (IBM).

### Enzyme-Linked Assays of Metabolites

Enzymatic assays were carried out on extracts from fully expanded leaves as described previously (Dyson *et al.* , 2016). Starch, sucrose and glucose, and malate were measured using total starch (Method E), sucrose D-glucose, and l-malic acid assay kits (Megazyme), respectively. To measure fumarate, the malate kit was modified to include an extra independent reaction step using 2 units fumarate hydratase enzyme (Sigma). Data were analysed using Analysis of Variance, followed by Tukey post-hoc tests, in SPSS (IBM).

### Proteomic analysis of plant material

Extraction of leaf proteins and analysis of protein content using gel-free LC-MS/MS was carried out as described by Miller *et al.* (2017). Briefly, frozen ground leaf samples (4 replicates per treatment) were extracted in a buffer containing Rapigest. After reduction, alkylation and trypsin digestion, samples were analysed by LC-MS/MS using an UltiMate® 3000 Rapid Separation LC (RSLC, Dionex Corporation, Sunnyvale, CA) coupled to an Orbitrap Elite mass spectrometer (Thermo Fisher Scientific, MA, USA). Raw data were analysed in Progenesis and peptide assignments were made using Mascot. A principal component analysis (PCA) was performed in the R software package using log<sub>2</sub> scaled protein intensities. Proteins were considered to have significantly changed in abundance when a p value of  $<0.05$  was reached, with a fold change of 1.2 or greater. For hierarchical clustering analysis, log<sub>2</sub> scaled protein values were used. Hierarchical clustering was performed using Euclidean distance and the complete linkages method. For heatmap/cluster analysis, fold change data were calculated relative to the wild type Col-0 at LL and log<sub>2</sub> scaled. A heatmap was then generated using the heatmap.2 package in R software, using the default settings.

### Metabolic Modelling

We adapted a metabolic model by Arnold and Nikoloski (2014) to allow for the diurnal accumulation of carbon compounds. Specifically, we ensured that cytosolic fumarate could be produced from cytosolic malate and added “export reactions” to the model (describing diurnal storage pools) for malate, fumarate and starch in addition to the already existing sucrose export. We generated four models: Wild type Col-0 in 20°C and 4°C conditions and *fum2* in 20°C and 4°C conditions. We constrained the models using metabolite assays such that the beginning of day concentrations of fumarate, malate, and starch subtracted from their respective end of day concentrations equated to the diurnal flux over the eight-hour photoperiod. Furthermore, we assumed a constant rate of photosynthesis (Dyson *et al.* , 2016) throughout the day and converted the measured rates of photosynthesis to diurnal fluxes of carbon intake. We then used proteomics data to further constrain the upper bounds of the flux reactions (Ramon, Gollub, & Stelling, 2018). For each metabolic reaction we checked whether all of the corresponding proteins were available in the data set; if so, then those reactions were given an upper bounds of additive value of all of the identified proteins in case multiple isoforms exist.

Given that the proteomics data is relative and not quantitative we scaled all of the proteomics constraints such that we were able to obtain model solutions across all four models. We used single flux solution, from a flux balance analysis maximizing carbon assimilation via Rubisco within feasible model constraints, in order to eliminate non-essential reactions which generate loops within the model, using the `loopless` function in the *cobra* (version 0.10.1) package. We then conducted flux sampling using the CHRR algorithm in the MATLAB toolbox as outlined in Herrmann, Dyson, Vass, Johnson, and Schwartz (2019).

All models, code and data used to conduct the computational analyses are available at <https://github.com/HAHerrmann/FluxSamplingCol0Fum2> and have been archived in Zenodo (DOI: 10.5281/zenodo.3366934).

## Network Analysis

We converted the metabolic model to a metabolite-metabolite graph of primary carbon metabolism using the method of Ranganathan and Maranas (2010). A full list of the nodes and edges is available on Zenodo (DOI: 10.5281/zenodo.3366934). We then used the `networkx` (version 1.10) package in python in order to iteratively identify pathways with fewer than 20 nodes connecting Rubisco and fumarate node. We checked these pathways against the flux sampling solutions of the Col-0 models and identified pathways which carried a flux substantial enough to account for fumarate accumulation in the model.

## Results

### Acclimation of both photosynthesis and respiration to cold are impaired in plants lacking FUM2

Plants of the wild type *Arabidopsis*, accession Col-0 and a mutant in the same background, *fum2.1*, were grown for 8 weeks at a daytime temperature of 20°C, before being transferred to a growth cabinet with the same light conditions, but with a temperature of 4°C. Photosynthetic capacity ( $P_{\max}$ ; measured at 20°C in saturating light and CO<sub>2</sub>) of these plants was measured over the following 9 days (Figure 1a). Prior to transfer to low temperature,  $P_{\max}$  of Col-0 was slightly higher than that of *fum2.1*. Following one day at low temperature, the capacity for photosynthesis in Col-0 increased.  $P_{\max}$  continued to increase over the following days, rising to a new steady state approx. 50% higher than the starting value by Day 7 of treatment. This indicates that dynamic acclimation of photosynthesis is occurring in response to cold, with a new steady-state being reached within 7 days under our conditions. In contrast, the  $P_{\max}$  of *fum2.1* did not vary over the course of the experiment, confirming previous evidence that mutants lacking FUM2 are defective in cold acclimation (Dyson *et al.*, 2016).

Measurements of the rate of gas exchange in plants under *growth conditions*, performed towards the end of the first day of cold, showed that transfer to cold resulted in a small but significant inhibition of both photosynthesis and respiration at the end of the first day of exposure to cold (ANOVA,  $P < 0.05$ ; Figure 1b,c). In Col-0, acclimation of both parameters occurred, such that values recorded at 4°C in plants exposed to cold for 7 days did not differ significantly from those recorded at 20°C prior to acclimation. In contrast, in *fum2.1*, no recovery occurred. This shows that either fumarate accumulation or FUM2 protein, is essential not only for the acclimation of photosynthesis but also of respiration to cold.

### Acclimation to cold changes partitioning of metabolites between sinks

In plants, diurnally-produced organic carbon can be directly exported from the leaf, used in cellular respiration, or stored in a variety of forms. In *Arabidopsis*, the principal leaf carbon stores are starch and organic acids, especially fumarate and malate (Chia, Yoder, Reiter, & Gibson, 2000; Zell *et al.*, 2010). When plants are exposed to cold for a single photoperiod, the accumulation of both starch and organic acids increases (Dyson *et al.*, 2016). We measured the beginning and end of photoperiod concentrations of starch, fumarate and malate in Col-0 and *fum2.1* on each of the 7 days following transfer to cold (Figure 2). The diurnal accumulation of these metabolites shows clear evidence of acclimation in both genotypes. Starch accumulation was greater than 20°C on the first day of cold and continued to increase each day, until Day 4 of cold treatment, in both wild type and mutant plants (Figure 2a). The amount of starch seen at the end of

day was higher in *fum2.1* than in Col-0 throughout the experiment, with the absolute difference between genotypes being approximately constant. In Col-0, essentially all starch accumulated during the day was mobilised overnight throughout the acclimation period, however in *fum2.1*, a small amount of starch was retained in the leaf at dawn after the third day of cold treatment.

In Col-0, there was an increase in the amount of fumarate accumulated each day through the acclimation period (Figure 2b). This was accompanied by an increase in the accumulation of malate (Figure 2c), such that these acids represented an increased proportion of total stored carbon. In *fum2.1*, the amount of fumarate was always substantially lower than in Col-0 and at no point in the experiment was there evidence of a diurnal accumulation of fumarate. End-of-day malate concentrations were increased on the first day of cold in *fum2.1* but then fell the following day, before rising again towards the end of the treatment period in response to cold treatment.

Arabidopsis does not accumulate substantial amounts of sucrose in its leaves under most conditions, but sucrose is known to play an important role in freezing tolerance (Stitt & Hurry, 2002). We assayed leaf sucrose and glucose content in response to cold treatment (Figure S1). At 20°C, there is a significant diel cycle in sucrose content, however, as plants acclimated to cold, this cycle was lost, with beginning of day sucrose content increasing and end of day content decreasing progressively through the week. At the end of the cold treatment, *fum2.1* contained slightly more sucrose than Col-0 but in neither case was a significant diel variation seen.

To understand better how the partitioning of carbon between different pools varies in response to acclimation, we combined data from Figures 1-2, S1 and from Dyson *et al.* (2016) to perform a carbon budget audit (Figure 3). The accumulation of starch, sucrose, fumarate and malate were estimated as the difference in beginning and end of day concentrations (Figure 2, S1). The rate of photosynthesis was measured under growth conditions at intervals through the photoperiod (Dyson *et al.*, 2016) and used to calculate the integrated daily photosynthesis. Diurnal respiration was estimated based on gas exchange measurements during short interruptions in irradiance (Figure 1c) and assumed to be constant through the photoperiod.

In Col-0 at 20°C, stored carbon accounted for approx. 1/3 of total fixed carbon. When combined with the estimated rate of daytime respiration, slightly over half of the fixed carbon could be accounted for. The remaining carbon is assumed to be exported from the leaf or remain in the form of other organic compounds not measured here. It is assumed that the bulk of this carbon will be exported, consistent with estimates by Lundmark *et al.* (2006). Plants of *fum2.1* at 20°C showed similar photosynthesis and respiration to Col-0. Although they do not accumulate fumarate, the proportion of total carbon stored as organic acid was similar to that seen in Col-0, with an increased accumulation of malate. Combining this with the increase in starch accumulation, we conclude that total unaccounted carbon, primarily diurnal export, is lower in *fum2.1* than in Col-0.

During the first day of exposure to cold, there were notable changes in carbon distribution between different sinks (Figure 3b,e). Total fixed carbon was lower on Day 0 (first day) of cold due to the lower rate of photosynthesis (Figure 1). In both genotypes, the total amount of fixed carbon we were able to account for increased, implying that diurnal carbon export is probably inhibited. Unaccounted carbon was still greater in Col-0 than in *fum2.1*. When plants were cold-acclimated for 7 days, this effect became more marked (Figure 3c,f). From this, we conclude that there is a substantial inhibition of diurnal carbon export from the leaf in cold acclimated plants of both genotypes. Given that all metabolite pools retain a diel turnover, we conclude that acclimation to cold involves a shift from diurnal carbon export to nocturnal processes.

### **Acclimation to cold involves changes in the proteome of both Col-0 and *fum2.1***

In a previous study of dynamic acclimation of photosynthetic capacity, in response to increased light, we saw that acclimation entails an increase in enzyme concentrations involved in multiple metabolic processes (Miller *et al.*, 2017). In Col-0, cold exposure for 7 days resulted in a significant increase in leaf protein content (Figure 4a), with an approx. 30% increase in protein content per unit fresh weight of leaf. In *fum2.1*, protein content did not change significantly. Nevertheless, analysis of the proteome shows that there were

changes occurring in both Col-0 and *fum2.1*, albeit to a much smaller extent in the latter. We were able to estimate the relative abundance of 2427 polypeptides, based on a minimum of 3 unique peptides per protein. Principal Component Analysis of proteomic data indicates that the proteomes of Col-0 and *fum2.1* differ already under 20°C conditions, however there is a clear separation of cold acclimated plants from their corresponding 20°C controls in both genotypes (Figure 4b). Cluster analysis was performed using data from the 2015 proteins which showed significantly altered expression in one of more conditions. As expected, given the total increase in protein, the most common response to cold is for proteins to increase in Col-0 but less so or not at all in *fum2.1* (Figure 4c Clusters 1, 4). A far smaller cluster of proteins increased in both genotypes following acclimation (Cluster 2) whilst a few proteins decreased in response to cold in *fum2.1* (Cluster 3).

Examination of the relative concentration of proteins involved in the photosynthetic electron transport chain demonstrated that only subtle changes were occurring (Table S1). There were increases in the relative abundance of various peripheral PSII proteins, including isoforms of PSBS, and in PSB29, which has been implicated in PSII assembly (Keren *et al.*, 2005), however components of the PSII core did not change significantly in response to cold. Amongst the proteins of the photosynthetic electron transport chain, 2 of the 4 detected Cyt b<sub>6</sub>f complex subunits increased significantly in Col-0, while measurements for the other subunit were too variable to allow a confident assessment of changes in abundance. Overall, this suggests a tendency to increase cytochrome b<sub>6</sub>f abundance in Col-0, whilst in *fum2.1* there is no evidence for a change in the abundance of this complex. While plastocyanin showed no change in abundance in either genotype, the only detected ferredoxin isoform increased in both genotypes, as did one of the four detected FNR isoforms. 4 of the detected 8 ATP synthase subunits were upregulated in Col-0, whilst 2 showed a significant change in *fum2.1*. Taking these data overall, we conclude that there were no changes in photosystem stoichiometry in response to cold in either genotype and that changes in electron transport proteins in Col-0 were either reduced or absent in *fum2.1*. There were however consistent and significant differences between the genotypes both in warm and cold conditions, with a greater abundance of subunits of all complexes being seen in Col-0.

In contrast to the components of the photosynthetic electron transport chain, changes in the enzymes associated with the Benson Calvin cycle gave a clearer and more consistent pattern of response (Figure 5). The CO<sub>2</sub> fixing enzyme, Rubisco, is by far the most abundant protein in the leaf. We were able to quantify the chloroplast-encoded large subunit (RBCL) and 2 isoforms of the nuclear-encoded small subunit, RBCS. All increased significantly in Col-0 in response to cold, with a mean 1.8-fold increase in relative abundance. In *fum2.1* there was no significant change in RBCL abundance. One isoform of RBCS increased significantly, whilst the other decreased to a similar extent. Combining data from both isoforms, there was no significant change in RBCS abundance. For other reactions associated with the Benson Calvin cycle, we were able to quantify a total of 20 distinct proteins, including isoforms of specific enzymes. In Col-0, 14 of these significantly increase, whilst 5 decreased. In *fum2.1*, although 6 enzymes involved in the Benson Calvin cycle came out as significantly increased, the overall extent of this change was lower.

Across other major metabolic pathways – including starch and sucrose synthesis, glycolysis and the tricarboxylic acid cycle, similar patterns of acclimation were observed, with most proteins increasing in the cold in Col-0 and *fum2.1* but to a lesser extent in the latter case (Table S1). In the sucrose synthesis pathway, most enzymes increased their concentration in response to cold in both genotypes, but with the relative abundance of these tending to be lower in *fum2.1* (Figure S2). A notable exception to this was sucrose phosphate phosphatase, which did not increase in *fum2.1*.

To summarise, acclimation of photosynthesis to low temperature in Col-0 involves an increase in the abundance of some electron transfer proteins, though not reaction centres, and substantial changes in the amount of a broad range of Benson Calvin cycle enzymes. These changes are largely or completely absent in *fum2.1*. Changes in the proteome across metabolism show a similar tendency but a different extent in other metabolic pathways. These data indicate that fumarate accumulation or FUM2 protein or activity plays a central role in high-level processes regulating acclimation of metabolism.

**Metabolic modelling shows that cold induces an alteration in carbon export from the chloroplast which is perturbed in *fum2.1***

Results presented here show that acclimation to cold results in a substantial change in the metabolism of Col-0 plants, with a shift from diurnal to nocturnal carbon export from the leaf and an increase in leaf diurnal carbon storage. In *fum2.1* a similar shift occurs, but with a different distribution of carbon between pools. Plants of *fum2.1* carry out significantly less photosynthesis in the cold but retain a greater proportion of fixed carbon in the leaf. Although the protein changes in *fum2.1* are less marked than in Col-0, there is nevertheless evidence of metabolic changes over the week, implying that a form of acclimation is occurring. To better understand the factors underlying these changes in the two genotypes, we adopted a modelling approach.

Modelling was performed using flux sampling (Herrmann, Dyson, *et al.*, 2019) based on a modified version of the model of Arnold and Nikoloski (2014; see Methods for details). Previous measurements have shown that the accumulation of carbon storage pools is approximately linear across the photoperiod (Smith & Stitt, 2007; Dyson *et al.*, 2016), and so the model was constrained according to the rates of photosynthesis and the mean estimated rates for starch, fumarate and malate accumulation. Flux to export was not constrained. Although the proteomics data obtained do not provide absolute quantitation, observed changes are relative to one another and were used to impose further flux constraints onto the model (Ramon *et al.*, 2018). We scaled the proteomic data to set feasible upper bounds on all reactions with corresponding proteins. Upper bounds for reactions associated with more than one gene product were set to the total sum of all associated proteins only if data for all those proteins was available. In total we constrained the upper bounds of 101 reactions. Because protein presence does not necessarily equate to enzymatic activity we set the lower bounds of reversible reactions to the negative value of the upper bounds and the lower bounds of non-reversible reactions were set to 0. We generated four different models of different constraint types. This included two models of Col-0, one constrained with the experimental results obtained from plants grown in 20°C conditions and one constrained with the experimental results of 7-day cold-acclimated plants. The same was done for the *fum2.1* genotype, with the addition that the cytosolic fumarase reaction was deleted in those models to simulate the knockout. Constraining the model using the proteomic data allowed us to analyse the above observed difference in Col-0 and *fum2* plants in response to cold, including changes in the electron transport proteins and Benson Calvin cycle enzymes, in a system context.

In order to determine the shortest feasible pathways by which assimilated carbon can be converted to cytosolic fumarate, we iteratively applied the min-path method (Ranganathan & Maranas, 2010) and validated all pathways with 20 or fewer metabolites against the flux sampling results in order to see whether they were carrying a significant flux under the given model constraints. The flux sampling results confirmed two of these pathways to be feasible in the Col-0 and *fum2* 20°C models (Figure 6). These pathways differ in terms of their relative consumption of ATP and NADPH. Activity of Rubisco produces 3-phosphoglyceric acid (PGA) from ribulose-1,5-phosphate and CO<sub>2</sub>. PGA can then be converted to triose phosphate (TP) in reactions requiring ATP and NADPH. There are two forms of TP (glyceraldehyde-3-phosphate and dihydroxy acetone phosphate); when exporting either of the two forms from the chloroplast in our analysis we obtained the same results and therefore refer to the two forms collectively as TP export. TP is exported from the chloroplast in exchange for inorganic phosphate by the triose phosphate translocator (TPT). Conversion of TP to fumarate includes the reconversion of TP to PGA in the cytosol. The PGA is then carboxylated and reduced to form malate. The TPT is also capable of exporting PGA directly, eliminating the reduction reaction in the chloroplast.

We assessed how the export of PGA versus TP from the chloroplast varies under changing conditions using flux sampling (Figure 7). In models of 20°C conditions, most carbon is exported from the chloroplast in the form of TP, with the *fum2* model tending to have higher PGA export (Figure 7 a,e). In the Day 0 cold model, where the rate of photosynthesis is restricted, PGA export is increased and TP export decreased in Col-0, whilst in *fum2* both show a tendency to be reduced (Figure 7 b,f). In Col-0 plants acclimated to cold (“Day 7 – 4°C”), where the rate of photosynthesis recovers (Figure 1b), PGA export is modelled to decrease relative to Day 0, while TP export is largely unaffected (Figure 7 c,g). At the same time, in the *fum2* model, PGA export is largely absent.

Previous experimental data have indicated that the ATP/NADPH ratio increases at low temperature in *Arabidopsis* (Savitch *et al.*, 2001), possibly reflecting changes in the ratio of cyclic to linear electron transport (Clarke & Johnson, 2001). To simulate this, we ran Col-0 and *fum2* versions of the model in which we restricted NADPH production (simulating a restriction in electron transport capacity). When limiting the NADPH production in the cell (by setting the flux value of the NADPH producing reaction to the minimum feasible value) a similar effect to the initial cold response was achieved: PGA export increases (Figure 7d,h). By implementing cyclic electron flow in the model, it makes sense that reducing the rate of photosynthesis will have a similar effect to limiting the NADPH production. Whilst metabolic modelling suggests an increase in PGA:TP export from the chloroplast under cold and NADPH-limited conditions, this effect disappears in the *fum2* models. In fact for *fum2* PGA export is potentially highest in 20°C conditions (Figure 7a).

## Discussion

Previous work has shown that the ability to acclimate photosynthesis and metabolism to changes in the abiotic environment plays an important role in determining plant fitness and seed yield (Athanasidou *et al.*, 2010). We have seen that acclimation of photosynthetic capacity to both light and temperature involves metabolic signalling, as evidenced by knock outs of either the glucose 6 phosphate/phosphate translocator GPT2 or of the cytosolic fumarase FUM2 being deficient in their acclimation responses (Athanasidou *et al.*, 2010; Dyson *et al.*, 2015; Dyson *et al.*, 2016; Miller *et al.*, 2017). Recently, Weise *et al.* (2019) confirmed that the increase in GTP2 transcripts in response to environmental change is linked to TPT export and that this link is an important feature of day-time metabolism. Here we show that cold acclimation involves a reconfiguration of diel carbon metabolism of the leaf, with a major shift in the ratio of diurnal carbon leaf storage to export. Plants acclimated to cold retain more carbon in the leaf during the day and therefore must export more overnight. Furthermore, we provide evidence from metabolic modelling that acclimation responses may depend on the form of carbon export from the chloroplast. Specifically, we propose that the PGA:TP chloroplast export ratio provides a novel potential retrograde signal, which may drive aspects of acclimation responses both in the chloroplast and the wider cell.

Earlier studies on the cold acclimation of photosynthesis in *Arabidopsis* highlighted the importance of sucrose synthesis and, specifically, the activity of sucrose phosphate synthase (Stitt & Hurry, 2002; Strand, Foyer, Gustafsson, Gardstrom, & Hurry, 2003). It was suggested that phosphate recycling is impaired at low temperature, due to the accumulation of sugar phosphates, such as glucose-6-phosphate, fructose-1,6-bisphosphate and fructose-6-phosphate. Evidence from the *fum2.1* mutant speaks against a direct role for phosphate in controlling the acclimation of photosynthetic capacity— non-acclimating *fum2.1* plants show higher levels of sugar phosphates on the first day of cold than do Col-0 plants, and should therefore have a stronger photosynthetic acclimation signal (Dyson *et al.*, 2016). If phosphate is a signal for acclimation, fumarate accumulation must play a role down-stream of this, preventing acclimation despite the signal. This conclusion is further supported here. Measurements of the major sugar phosphates involved in sucrose synthesis (Figure S2) shows that these tend to increase as a result of acclimation. There is however no persistent significant difference in the concentrations of these in the different genotypes. Phosphate may well play a role in some of the short-term regulatory responses seen on exposure to cold, however (Hurry *et al.*, 2000).

Regardless of the role of phosphate in cold sensing, diurnal flux to sucrose is clearly an important part of the cold response. On the first day of exposure to cold, the estimated maximum possible flux to sugar export dropped significantly, compared to plants maintained at 20°C (Figure 3). This effect might be explained by a drop in sink strength, however, if this is the case, then this is not alleviated by acclimation at the whole plant level. At the end of the acclimation period, the proportion of carbon retained in the leaf during the day is even lower than on the first day of acclimation. If the reduction in daytime export is indeed sink limited, it is unlikely to be a consequence of the overall capacity of sinks since, over the diel cycle, there was no evidence of progressive accumulation of fixed carbon in the leaf. Thus, nocturnal processes, including export from the leaf or increased nocturnal respiration, compensate for diurnal export.

Nocturnal metabolism of leaves remains poorly understood. At night, there is a highly controlled mobilisation of starch, which is maintained at an approximately constant rate through the night (Graf & Smith, 2011;

Smith & Stitt, 2007). At the same time, our data show that stored organic acids are also mobilised. Carbon export in *Arabidopsis* is thought to largely be in the form of sucrose, however it is not clear in detail how this is synthesised, either from starch or organic acids. Starch breakdown involves the formation of maltose (di-glucose) and glucose molecules, which are exported from the chloroplast. If synthesis of sucrose follows the same pathway as in the daytime, the glucose would need to be phosphorylated, by hexokinase, before being incorporated into sucrose. Sucrose phosphate synthase (SPS) is the major enzyme responsible for the diurnal synthesis of sucrose (Huber & Huber, 1996). It is not clear why this pathway would operate more efficiently at night than it does during the day. It may therefore be that an alternative pathway for sucrose synthesis at night exists. We did observe a substantial increase in the concentration of the main isoform of sucrose synthase (SS) following cold acclimation (Table S1). SS produces sucrose from the reaction of UDP-glucose with fructose, in contrast to SPS which reacts UDP-glucose with fructose-6-phosphate (Stein & Granot, 2019). SS would in theory represent a lower energy pathway to generate sucrose from hexoses. SS is generally believed however to operate in the direction of sucrose breakdown, releasing glucose for metabolic processes. It is therefore not obvious why SS would normally be present in mature leaves, which are net sources for carbon, and which do not store sucrose to a significant degree. It is possible though that night-time sucrose synthesis may involve SS.

The synthesis of fumarate has an impact on diurnal carbon export from the leaf which cannot be explained by a reduction in storage capacity. At 20°C, *fum2.1* plants maintain a similar photosynthetic rate but store a larger proportion of total carbon in the leaf than do wild type Col-0 plants. Although fumarate accumulation is inhibited, this is largely compensated for by increased accumulation of malate. At the same time, starch storage is greater. As in Col-0, short term exposure to cold increases this effect and following 7 days acclimation, only a very small proportion of fixed carbon is exported during the day.

The role of fumarate accumulation in *Arabidopsis* leaves is not, we conclude, a simple carbon sink effect; it is affecting the overall distribution of carbon between different storage pools in ways that cannot simply be explained by a loss of storage capacity. In order to better understand the possible processes affected by fumarate accumulation, we adopted a modelling approach. Using a network analysis of a metabolite-metabolite graph (see methods for details), we identified several potential pathways for fumarate synthesis. When modelling potential flux solutions for these pathways, only two of the identified pathways carried a significant flux. These involve export of fixed carbon from the chloroplast in the form of either phosphoglyceric acid (PGA) or triose phosphate (TP – glyceraldehyde-3-phosphate and dihydroxy acetone phosphate). These compounds are all transported by the same translocator – the triose phosphate translocator (TPT) – which is reported to have very similar transport properties for these different compounds (Knappe, Flugge, & Fischer, 2003). Comparison of plants lacking one or other of these exports is therefore not possible via traditional experimental approaches such as reverse genetics or using inhibitors.

The main modelling approaches adopted to understand metabolism can be classified as kinetic or constraint-based models (Herrmann, Schwartz, & Johnson, 2019). Kinetic models require detailed kinetic information about enzymes and are computationally expensive, limiting the complexity of systems which can be analysed. Constraint based models can be much more complex, however the most widely used approach, flux balance analysis, has the disadvantage that it requires the assumption of one or more objective functions – model solutions are established based on a presumed cellular goal, often maximising a portmanteau function describing “biomass”. This introduces a researcher bias into the modelling process. Recently, we highlighted an alternative approach, flux sampling, which eliminates this bias. Rather than using an objective function, the entire solution space of the model is explored and a frequency distribution of different flux solutions considered for each metabolic reaction. This allows us to define the range and the likelihood of possible solutions.

Here we have applied flux sampling to gain an understanding of the impact of fumarate synthesis on wider metabolism. Building on a published model (Arnold & Nikoloski, 2014), we show that export of carbon from the chloroplast can occur either as PGA or TP. The model was constrained using experimental data: carbon input and fluxes to major storage sinks were set according to measured physiological parameters, and the

relative capacity of individual reactions constrained in proportion to changes in the proteome (Table S1). The broad validity of this model comes from the observation that carbon export, which was not constrained, varied in a way consistent with the experimental data (Figure 3, Figure S3). Based on this, we conclude that the proportion of carbon exported as PGA is an initial response to cold in Col-0 plants. Furthermore, we were able to demonstrate that, in the model, the ratio of PGA:TP export varies as a function of NADPH supply from the photosynthetic electron transport chain. Limitation in NADPH is known to be an early response to low temperature, as flux through the linear electron transport chain decreases (Clarke & Johnson, 2000). At the same time, cyclic electron flow at low temperature will tend to increase the ATP:NADPH ratio. NADPH in the chloroplast is essential for the conversion of PGA into TP. Limited NADPH supply will tend to favour PGA export. Thus, the relative export of PGA and TP from the chloroplast represents a potential new retrograde signal which signal to the nucleus the redox state of the chloroplast.

PGA in the cytosol is converted to phospho-*enol*-pyruvate (PEP) and then carboxylated by PEP carboxylase to form oxaloacetate (OAA). OAA is in turn reduced by malate dehydrogenase to form malate. In our modelling, the net accumulation of malate and fumarate was constrained to experimental levels, nevertheless, it remains unclear why flux to malate would be biologically different to flux to fumarate, given that these acids exist in equilibrium, catalysed by fumarase. One possible explanation though lies in the regulation of PEP carboxylase, which is subject to feedback inhibition by malate. If malate accumulates, this is liable to feedback to inhibit its own synthesis. Removing malate, converting it to fumarate, ensures that this pathway does not become limiting. This may be essential to ensure that fluxes away from PGA are not sink limited, so ensuring the PGA concentrations in the cytosol reflect the rate of export and do not accumulate over the photoperiod.

In conclusion, we have shown that the ability to accumulate fumarate in Arabidopsis leaves has wide-ranging impacts on diurnal carbon partitioning in the leaf. Lack of fumarate synthesis results in widespread differences being seen across the proteome and prevents the acclimation of photosynthetic capacity to low temperature. Fumarate accumulation is important in facilitating diurnal carbon export from the leaf. Low temperatures inhibit diurnal sucrose export and this effect is exacerbated in plants lacking fumarate accumulation. Modelling of leaf metabolism suggests that the relative export of PGA and TP may be an important retrograde signal reflecting the redox poise of the chloroplast.

**Acknowledgements:** We would like to thank Drs David Knight, Ronan O’Cualain and Julian Selley (University of Manchester) for their help with the proteomic analysis. This work was supported by a grant from the Biotechnology and Biological Sciences Research Council (BBSRC; BB/J04103/1). HAH and MAEM were supported BBSRC studentships (BB/M011208/1).

## References

- Armstrong, A. F., Logan, D. C., Tobin, A. K., O’Toole, P., & Atkin, O. K. (2006). Heterogeneity of plant mitochondrial responses underpinning respiratory acclimation to the cold in Arabidopsis thaliana leaves. *Plant, Cell & Environment*, 29 (5), 940-949. doi:10.1111/j.1365-3040.2005.01475.x
- Arnold, A., & Nikoloski, Z. (2014). Bottom-up Metabolic Reconstruction of Arabidopsis and Its Application to Determining the Metabolic Costs of Enzyme Production. *Plant Physiology*, 165 (3), 1380-1391. doi:10.1104/pp.114.235358
- Athanasiou, K., Dyson, B. C., Webster, R. E., & Johnson, G. N. (2010). Dynamic acclimation of photosynthesis increases plant fitness in changing environments. *Plant Physiology*, 152 , 366-373. doi:http://www.plantphysiol.org/cgi/reprint/152/1/366
- Chia, D. W., Yoder, T. J., Reiter, W. D., & Gibson, S. I. (2000). Fumaric acid: an overlooked form of fixed carbon in Arabidopsis and other plant species. *Planta*, 211 (5), 743-751.
- Clarke, J. E., & Johnson, G. N. (2000). In vivo temperature dependence of cyclic and pseudocyclic electron transport in barley. *Planta* .

Dyson, B. C., Allwood, J. W., Feil, R., Xu, Y. U. N., Miller, M., Bowsher, C. G., . . . Johnson, G. N. (2015). Acclimation of metabolism to light in *Arabidopsis thaliana*: the glucose 6-phosphate/phosphate translocator GPT2 directs metabolic acclimation. *Plant, Cell & Environment*, *38* (7), 1404-1417. doi:10.1111/pce.12495

Dyson, B. C., Miller, M. A. E., Feil, R., Rattray, N., Bowsher, C. G., Goodacre, R., . . . Johnson, G. N. (2016). FUM2, a Cytosolic Fumarase, Is Essential for Acclimation to Low Temperature in *Arabidopsis thaliana*. *Plant Physiology*, *172* (1), 118-127.

Fey, V., Wagner, R., Brautigam, K., & Pfannschmidt, T. (2005, 2005). *Photosynthetic redox control of nuclear gene expression*. Paper presented at the International Botanical Congress, Vienna, AUSTRIA.

Graf, A., & Smith, A. M. (2011). Starch and the clock: the dark side of plant productivity. *Trends in Plant Science*, *16* (3), 169-175. doi:10.1016/j.tplants.2010.12.003

Herrmann, H. A., Dyson, B. C., Vass, L., Johnson, G. N., & Schwartz, J.-M. (2019). Flux sampling is a powerful tool to study metabolism under changing environmental conditions. *npj Systems Biology and Applications*, *5* (1), 32. doi:10.1038/s41540-019-0109-0

Herrmann, H. A., Schwartz, J.-M., & Johnson, G. N. (2019). Metabolic acclimation—a key to enhancing photosynthesis in changing environments? *Journal of Experimental Botany*, *70* (12), 3043-3056. doi:10.1093/jxb/erz157

Huber, S. C., & Huber, J. L. (1996). Role and regulation of sucrose-phosphate synthase in higher plants. *Annual Review of Plant Physiology and Plant Molecular Biology*, *47*, 431-444. doi:10.1146/annurev.arplant.47.1.431

Huner, N. P. A., Öquist, G., Hurry, V. M., Krol, K., Falk, S., & Griffith, M. (1993). Photosynthesis, photo-inhibition and low temperature acclimation in cold-tolerant plants. *Photosynthesis Research*, *37*, 19-39.

Hurry, V., Strand, Å., Furbank, R., & Stitt, M. (2000). The role of inorganic phosphate in the development of freezing tolerance and the acclimatization of photosynthesis to low temperature is revealed by the photo mutants of *Arabidopsis thaliana*. *The Plant Journal*, *24* (3), 383-396. doi:10.1046/j.1365-313x.2000.00888.x

Knappe, S., Flugge, U. I., & Fischer, K. (2003). Analysis of the plastidic phosphate translocator gene family in *Arabidopsis* and identification of new phosphate translocator-homologous transporters, classified by their putative substrate-binding site. *Plant Physiology*, *131* (3), 1178-1190.

Knight, M. R., & Knight, H. (2012). Low-temperature perception leading to gene expression and cold tolerance in higher plants. *New Phytologist*, *195* (4), 737-751.

Miller, M. A. E., O’Cualain, R., Selley, J., Knight, D., Karim, M. F., Hubbard, S. J., & Johnson, G. N. (2017). Dynamic Acclimation to High Light in *Arabidopsis thaliana* Involves Widespread Reengineering of the Leaf Proteome. *Frontiers in plant science*, *8*, 1239. doi:10.3389/fpls.2017.01239

Pracharoenwattana, I., Zhou, W. X., Keech, O., Francisco, P. B., Udomchalothorn, T., Tschoep, H., . . . Smith, S. M. (2010). *Arabidopsis* has a cytosolic fumarase required for the massive allocation of photosynthate into fumaric acid and for rapid plant growth on high nitrogen. *Plant Journal*, *62* (5), 785-795. doi:10.1111/j.1365-313X.2010.04189.x

Ramon, C., Gollub, M. G., & Stelling, J. (2018). Integrating -omics data into genome-scale metabolic network models: principles and challenges. *Essays in Biochemistry*, *62* (4), 563-574. doi:10.1042/ebc20180011

Ranganathan, S., & Maranas, C. D. (2010). Microbial 1-butanol production: Identification of non-native production routes and in silico engineering interventions. *Biotechnol J*, *5* (7), 716-725. doi:10.1002/biot.201000171

Ruelland, E., Vaultier, M.-N., Zachowski, A., & Hurry, V. (2009). Cold Signalling and Cold Acclimation in Plants. In J. C. Kader & M. Delseny (Eds.), *Advances in Botanical Research*, Vol 49 (Vol. 49, pp. 35-150).

Savitch, L. V., Barker-Astrom, J., Ivanov, A. G., Hurry, V., Oquist, G., Huner, N. P. A., & Gardestrom, P. (2001). Cold acclimation of *Arabidopsis thaliana* results in incomplete recovery of photosynthetic capacity, associated with an increased reduction of the chloroplast stroma. *Planta*, *214* (2), 295-303.

Smith, A. M., & Stitt, M. (2007). Coordination of carbon supply and plant growth. *Plant Cell Environ*, *30* (9), 1126-1149. doi:10.1111/j.1365-3040.2007.01708.x

Stein, O., & Granot, D. (2019). An Overview of Sucrose Synthases in Plants. *Frontiers in plant science*, *10* (95). doi:10.3389/fpls.2019.00095

Stitt, M., & Hurry, V. (2002). A plant for all seasons: alterations in photosynthetic carbon metabolism during cold acclimation in *Arabidopsis*. *Current Opinion in Plant Biology*, *5* (3), 199-206. doi:10.1016/s1369-5266(02)00258-3

Strand, A., Foyer, C. H., Gustafsson, P., Gardestrom, P., & Hurry, V. (2003). Altering flux through the sucrose biosynthesis pathway in transgenic *Arabidopsis thaliana* modifies photosynthetic acclimation at low temperatures and the development of freezing tolerance. *Plant Cell and Environment*, *26* (4), 523-535. doi:10.1046/j.1365-3040.2003.00983.x

Strand, A., Hurry, V., Gustafsson, P., & Gardestrom, P. (1997). Development of *Arabidopsis thaliana* leaves at low temperatures releases the suppression of photosynthesis and photosynthetic gene expression despite the accumulation of soluble carbohydrates. *Plant Journal*, *12* (3), 605-614.

Strand, A., Hurry, V., Henkes, S., Huner, N., Gustafsson, P., Gardestrom, P., & Stitt, M. (1999). Acclimation of *Arabidopsis* leaves developing at low temperatures. Increasing cytoplasmic volume accompanies increased activities of enzymes in the Calvin cycle and in the sucrose-biosynthesis pathway. *Plant Physiology*, *119* (4), 1387-1397. doi:10.1104/pp.119.4.1387

Talts, P., Parnik, T., Gardestrom, P. e. r., & Keerberg, O. (2004). Respiratory acclimation in *Arabidopsis thaliana* leaves at low temperature. *Journal of Plant Physiology*, *161* (5), 573-579. doi:https://doi.org/10.1078/0176-1617-01054

Walters, R. G. (2005). Towards an understanding of photosynthetic acclimation. *Journal of Experimental Botany*, *56* (411), 435-447.

Walters, R. G., & Horton, P. (1994). Acclimation of *Arabidopsis thaliana* to the light environment - changes in the composition of the photosynthetic apparatus. *Planta*, *195* (2), 248-256.

Weise, S. E., Liu, T., Childs, K. L., Preiser, A. L., Katulski, H. M., Perrin-Porzondek, C., & Sharkey, T. D. (2019). Transcriptional Regulation of the Glucose-6-Phosphate/Phosphate Translocator 2 Is Related to Carbon Exchange Across the Chloroplast Envelope. *Frontiers in plant science*, *10* (827). doi:10.3389/fpls.2019.00827

Zell, M. B., Fahnenstich, H., Maier, A., Saigo, M., Voznesenskaya, E. V., Edwards, G. E., . . . Maurino, V. G. (2010). Analysis of *Arabidopsis* with Highly Reduced Levels of Malate and Fumarate Sheds Light on the Role of These Organic Acids as Storage Carbon Molecules. *Plant Physiology*, *152* (3), 1251-1262. doi:10.1104/pp.109.151795

## Figure legends

**Figure 1:** Maximum capacity of photosynthesis (a), measured at 20degC under CO<sub>2</sub>- and light-saturating conditions at the end of each day of the acclimation period, for the Col-0 wild-type (circles) and the *fum2.1* mutant (triangles). Rates of net photosynthesis at 20degC (b) and respiration (c) measured as CO<sub>2</sub> exchange in growth conditions on Col-0 and *fum2.1* plants at 20degC (white) and at 4degC after the first day of transfer (dashed) and after seven days of transfer (grey). Error bars show standard mean error (n=3-5). Different labels on columns in (b) and (c) indicate significantly different values (ANOVA, P<0.05)

**Figure 2:** Concentrations of starch (a), fumarate (b) and malate (c) in leaves measured at the beginning (open symbols) and end (closed symbols) of the photoperiod in Col-0 (circles) and *fum2.1* (triangles) plants. Error bars show standard mean error (n=5-7).

**Figure 3:** Pie charts summarizing the distribution of diurnally fixed carbon, calculated from Figures 1-3 and data in Dyson et al. (2016) for Col-0 (a-c) and *fum2.1* (d-f) plants in control conditions (a,d), on the first day of cold treatment (b,e) and after one week of cold treatment (c,f). Beginning of day concentrations were subtracted from end of day concentrations to estimate total diurnal fluxes to different sinks. Values were normalized according to the number of fixed carbons per metabolite. Export (and other) values were calculated by subtracting all other values from the total diurnal carbon capture via photosynthesis. Data for “sugar”, which include sucrose and glucose, are included but are not visible on the scale of this figure.

**Figure 4:** Total protein concentrations (a) as calculated from Bradford assays. Different labels on columns indicate significantly different values (ANOVA,  $P < 0.05$ ) Principal component analysis (b) of the log<sub>2</sub> scaled protein intensities in leaves of Col-0 (circles) and *fum2.1* (triangles) plants measured in control conditions (open symbols) and after one week of cold treatment (closed symbols). Hierarchical clustering and heat-maps (c) of the log<sub>2</sub> scaled protein values and their fold changes relative to Col-0 controls (indicated by solid line), are shown for the two genotypes and conditions. Full proteomic dataset is available in Supplementary Table S1.

**Figure 5:** Summary of the relative abundance of proteins for the Benson-Calvin cycle enzymes of Col-0 (white bars) and *fum2.1* (grey bars) plants in control conditions (solid colours) and on Day 7 of 4degC treatment (hatched bars), as shown in the legend on the bottom left. RuBP (ribulose biphosphate), 3PG (3-phosphoglycerate), 1,3-BPG (1,3-bisphosphoglycerate), GA3P (glyceraldehyde 3-phosphate), DHAP (dihydroxy-acetone-phosphate), SDP (sedoheptulose-1,7-bisphosphate), FBP (fructose-1,6-bisphosphate), F6P (fructose-6-phosphate), SDP (sedoheptulose-1,7-bisphosphate), S7P (sedoheptulose-1-phosphate), Ru5P (ribulose-5-phosphate), X5P (xylulose-5-phosphate). Data represent the total summed signal for all unique detected peptides in each case, normalised as described in the Methods. Error bars represent the standard mean error, with different letters indicating significantly different values

**Figure 6:** The two shortest feasible pathways for producing fumarate in the cytosol, identified using a network analysis and flux sampling (see Methods and Materials for more details). The two pathways differ in the form of carbon exported from the chloroplast to the cytosol compartments. RuBP (ribulose biphosphate), PGA (3-phosphoglyceric acid), DPGA (2,3-diphosphoglyverate), TP (triose phosphate), 2PGA (2-phosphoglycerate), PEP (phosphoenolpyruvate carboxylase), Pyr (Pyruvate), OAA (Oxaloacetate), Mal (Malate), Fum (Fumarate).

**Figure 7:** Flux sampling results obtained from the Col-0 (black) and *fum2.1* (gray) models for the export of PGA (3-phosphoglyceric acid ; a-d) and the export of TP (triose phosphate; e-h) from the chloroplast. Models were constrained according to cold conditions (a,e), to control conditions but with the rate of photosynthesis on the first day of 4degC treatment (b,f) , to cold conditions on Day 7 of 4degC treatment (c,g) and to control conditions with the production of NADPH set to lowest feasible value (d,h). Each panel shows a frequency diagram, representing the frequency with which each solution value was achieved over repeated iterations of the modelling.

## Supporting Information

Table S1: List of quantified proteins. Gene code and protein name are shown in the columns “Accession” and “Description”, respectively. The number of identified peptides, which may be shared with other proteins, is shown in the column “Peptide count”. Proteins were quantified only when 3 or more non-redundant constituent peptides were quantified, the number of which is shown in the column “peptides used for quantitation”. After normalisation, the average relative abundance of each protein is shown. Individual comparisons between each condition are also shown, with P being less than 0.05. Data also available at <https://github.com/HAHerrmann/FluxSamplingCol0Fum2/blob/master/ExperimentalData/ProteinConc.xlsx> and stored under the Zenodo DOI:

**Figure S1:** Concentrations of sucrose (a) and glucose (b) in leaves, measured at the beginning (open symbols) and end (closed symbols) of the photoperiod in Col-0 (circles) and *fum2.1* (triangles) plants. Error bars show standard mean error.

**Figure S2:** Summary of the enzyme concentrations of the sucrose synthesis pathway of Col-0 (white bars) and *fum2.1* (grey bars) plants in control conditions (solid colours) and on Day 7 of 4degC treatment (hatched bars), as shown in the legend on the bottom left. TP (triose phosphate), FBP (fructose-1,6-bisphosphate), F6P (fructose-6-phosphate), G6P (glucose-6-phosphate), Tre6P (trehaolse-6-phosphate), G1P (glucose-1-phosphate), UDPG (uridine diphosphate glucose), S6P (sucrose-6-phosphate). Error bars represent the standard mean error, with different letters indicating significantly different values

**Figure S3:** Flux sampling results obtained from the Col-0 (black) and *fum2.1* (gray) models for the production of malate (a,f), fumarate (b,g), starch (c,h), export (d,i) and respiration (e,j) as predicted under control condition constraints (a-e) and seven days of 4degC conditions (f-j).

Figure 1

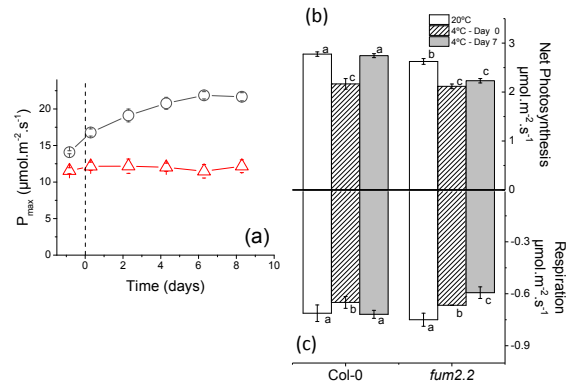


Figure 2

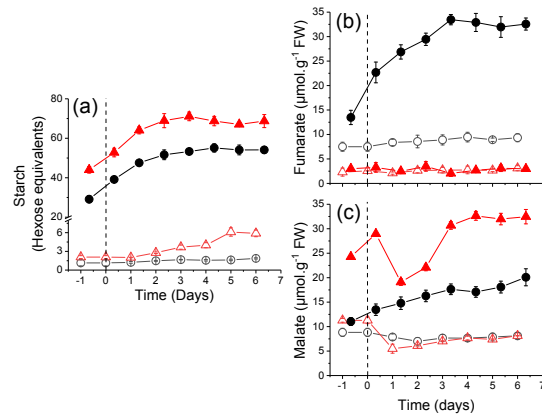


Figure 3

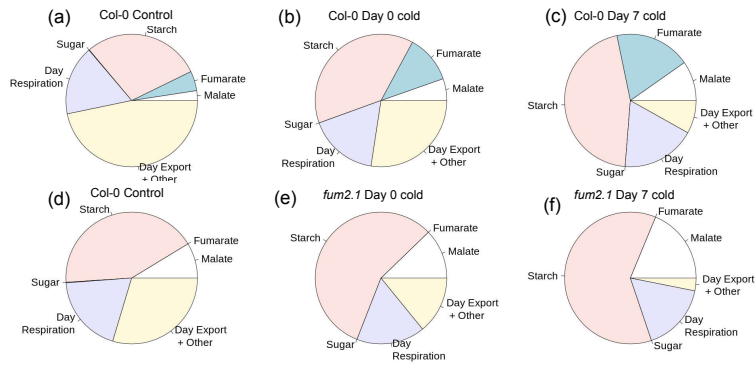


Figure 4

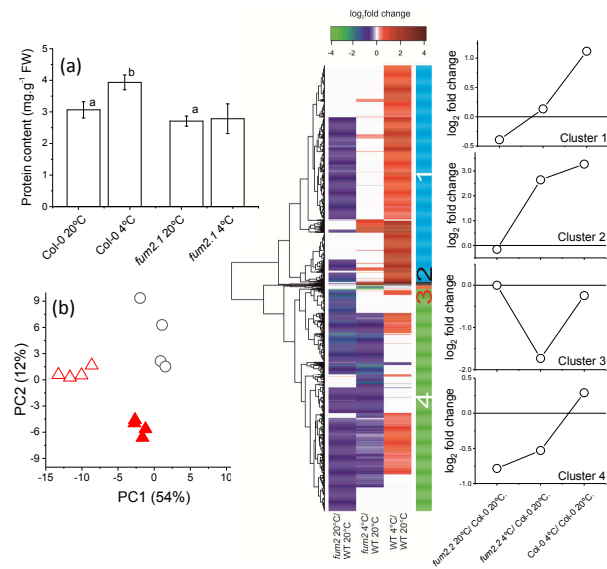


Figure 5

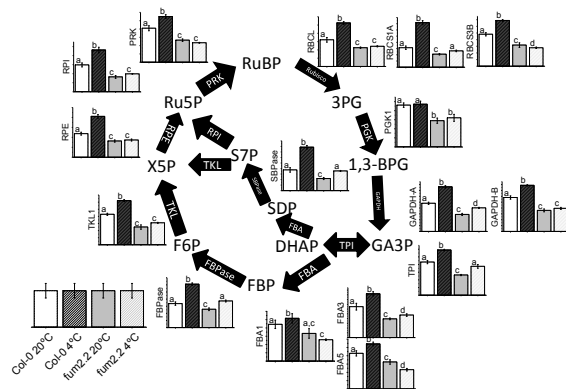


Figure 6

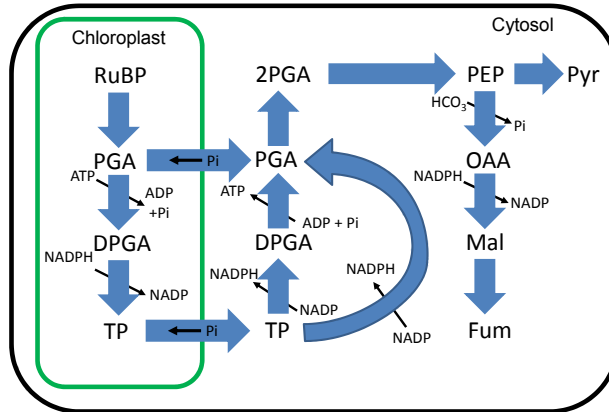


Figure 7

